Cellular/Molecular

Expression and Functional Phenotype of Mouse *ERG* K^+ Channels in the Inner Ear: Potential Role in K^+ Regulation in the Inner Ear

Liping Nie,[1] Michael Anne Gratton,[2] Karen J. Mu,[1] Judilee N. Dinglasan,[1] Weihong Feng,[1] and Ebenezer N. Yamoah[1]

[1]Center for Neuroscience, Department of Otolaryngology, University of California, Davis, Davis, California 95616, and [2]Department of Otorhinolaryngology, University of Pennsylvania, Philadelphia, Pennsylvania 19014

An outcome of the intricate K^+ regulation in the cochlear duct is the endocochlear potential (EP), ~80 mV, the "battery" that runs hair-cell transduction; however, the detailed molecular mechanisms for the generation of the EP remain unclear. We provide strong evidence indicating that the intermediate cells (ICs) of the stria vascularis (StV) express outward K^+ current that rectifies inwardly at positive potentials. The channel belongs to the *ether-a-go-go*-related gene (*erg*) family of K^+ channels. We cloned an ERG1a channel in the mouse inner ear (MERG1a). The cellular distribution of MERG1a in the cochlea displayed the highest levels of immunoreactivity in the ICs and modest reactivity in the marginal cells as well as in several extrastrial cells (e.g., hair cells). Functional expression of the StV-specific MERG1a channel reveals a current that activates at relatively negative potentials (approximately −50 mV) and shows rapid inactivation reflected as inward rectification at depolarized potentials. The current was sensitive to the methanesulfonanilide drug E-4031 (IC_{50}, ~165 nM) and the recombinant peptide rBeKm-1 (IC_{50}, ~16 nM), and the single-channel conductance in symmetrical K^+ was ~14 pS. The site of expression of MERG1a and its functional phenotype (e.g., modulation of the current by external K^+) make it one of the most likely candidates for establishing the high throughput of K^+ ions across ICs to generate EP. In addition, the property of the channel that produces marked K^+ extrusion in increased external K^+ may be important in shaping the dynamics of K^+ cycling in the inner ear.

Key words: **hearing; K^+ regulation; endocochlear potential; strial vascularis; long QT syndrome; delayed rectifier K^+ currents**

Introduction

A cadre of K^+ channels, pumps, and transporters confer K^+ cycling in the cochlear duct. The ensuing high throughput of K^+ across sensory and nonsensory cells generates the endocochlear potential (EP) (~80 mV), which boosts the receptor potential of hair cells to sculpt its acute sensitivity (Russell et al., 1989; Hudspeth, 1992; Wangemann, 2002). The prevalent hypothesis suggests that EP is generated in part by the high throughput of K^+ across the membrane of intermediate cells (ICs) and basal cells (BCs) of the stria vascularis (StV) and the uptake of K^+ from the interstrial space (IS) in the cochlear lateral wall (Salt et al., 1987; Carlisle et al., 1990). Because the inward rectifier, Kir4.1, is the main channel that has been identified in ICs, and because Ba^{2+}, a blocker of inward rectifier currents, reduces the EP (Hibino et al., 1997; Takeuchi et al., 2000), and finally because null deletion of the channel results in deafness, it has been inferred that Kir4.1 produces the outward K^+ flux necessary for the EP (Marcus et al., 2002). Kir4.1 may also facilitate a steep K^+ gradient between the ICs and the IS (Nie et al., 2005). Since the membrane potential of ICs is several millivolts positive to the reversal potential of K^+ (Takeuchi et al., 2000), it is unlikely that Kir4.1 alone controls the resting potential. The implications of these findings suggest that other K^+ channels may also confer the extrusion of K^+ across the IC membranes. Indeed, voltage-clamp recordings of ICs reveal clues about the presence of outward currents that show rectification at depolarized step voltages (Takeuchi et al., 2000).

The human *ether-a-go-go*-related gene (HERG) was cloned by homology to the *Drosophila* K^+ channel, ERG (Warmke and Ganetzky, 1994). It encodes a K^+ channel that mediates the cardiac repolarizing current I_{Kr}. Mouse ERG1 (MERG1a) is homologous to the full-length HERG1 (London et al., 1997). Although MERG1a is expressed in the heart and brain, MERG1b has been found only in the heart (London et al., 1997). Additional members of the ERG family are expressed exclusively in the nervous system (Shi et al., 1997). Moreover, HERG1 coimmunoprecipitates with MinK, encoded by KCNE1 and MinK-related protein 1 (MiRP1) (McDonald et al., 1997; Abbott et al., 1999), and the association of MinK to HERG increases the current amplitude (Yang et al., 1995). The interaction of the K^+ channel, KCNQ1, with HERG has also been shown *in vitro* and *in vivo*, suggesting that these channels are gleaned to form a delayed rectifier system in native cells (Ehrlich et al., 2004). Thus, an ensemble of several pore-forming α-subunits and auxiliary subunits may confer native K^+ currents.

In the inner ear, the expression of MinK and KCNQ1 in mar-

Received April 11, 2005; revised Aug. 6, 2005; accepted Aug. 8, 2005.

This work was supported by National Institutes of Health Grants DC07592 (E.N.Y.), DC04215 (E.N.Y.), and DC006442 (M.A.G.). L.N. was supported by grants from the National Organization of Hearing Research and the Sand Family Fund Grant in Auditory Science. We thank Dr. N. Chiamvimonvat and members of our laboratory for their constructive comments.

Correspondence should be addressed to Ebenezer N. Yamoah, Center for Neuroscience, Department of Otolaryngology, University of California, Davis, 1544 Newton Court, Davis, CA 95616. E-mail: enyamoah@ucdavis.edu.

DOI:10.1523/JNEUROSCI.1422-05.2005

 0270-6474/05/258671-09$15.00/0

ginal cells (MCs) of the StV has been demonstrated, and null deletion of either protein abolishes the EP (Vetter et al., 1996; Casimiro et al., 2004). Moreover, the role of HERG in the K^+ channel ensemble in the inner ear is unknown. We have identified MERG1a in the cochlear duct and vestibule with electrophysiology, reverse transcription (RT)-PCR, immunohistochemistry, and immunoelectron microscopy approaches. The cell-specific expression and properties of the channel suggest that MERG1a is poised to contribute to K^+ regulation in the inner ear.

Materials and Methods

Molecular identification and cloning of MERG1a in the mouse inner ear

Total RNA was extracted from microdissected mouse StV and organ of Corti (OC) tissue with an RNeasy Mini Kit (Qiagen, Hilden, Germany) and reverse transcribed to cDNA with SuperScript III reverse transcriptase according to the manufacturer's instructions (Invitrogen, San Diego, CA). RT-PCR was performed to investigate the expression of MERG1 in the inner ear with the primer pair merg-sense (merg-s; 5′-GGACCTCATCGTGGACATCATG-3′) and merg-antisense (merg-a; 5′-ACTCGGGCAGGGCCTTGCCCC-3′), which were designed from the mouse heart MERG1a sequence (GenBank accession number AF012868; amino acids 1689–3076). Then, the molecular identity of the PCR products was confirmed by sequencing. To clone the complete open reading frame of MERG1a from mouse inner ear, three RT-PCRs were performed with primer pairs based on a mouse MERG1a sequence (GenBank accession number AF012868): mergE1s, GCCACCATGCCGGTGCGGAGGGGCCA; mergE1a, GGACAGGACCTGGGTGACCTT (position 321–1470); mergE2s, GACCCACAATGTCACCGAG; mergE2a, AGATGAAGTAGAGGGCAGTAAG (position 1430–2680); mergE3s, GTTCAAGACCACACATGC; and mergE3a, GGATATCACTAACTGCCTGGATCTG (position 2603–2819). PCR products were then cloned into a pCRII-TOPO vector (Invitrogen) and sequenced. The full-length MERG1a was assembled from these three overlapped PCR fragments in the pNLR vector and used for heterologous expression in mammalian [Chinese hamster ovary (CHO)] cell lines and *Xenopus* oocytes (Nie et al., 2004).

Immunohistochemistry

Sedated [Avertin (2,2,2-tribromoethanol); 300 μg/gm body weight, i.p.] 129 × 1/SvJ mice were transcardially perfused with 10 ml of PBS followed by 10 ml of 4% paraformaldehyde in 0.1 M phosphate buffer. The temporal bones were removed, and the cochlea was perfused via the oval and round windows. The temporal bones were then immersed in fixative for 60 min. After fixation, the cochleas were decalcified (120 mM EDTA, pH 7.0; 24 h; 23°C), dehydrated in a graded ethanol series, embedded in paraffin (Paraplast; McCormick Scientific, St. Louis, MO), and sectioned (5 μm) in the mid-modiolar plane. The antibody used was a polyclonal anti-ERG1 channel antibody that reacts with highly conserved residues 11145-1159 (LTSQPLHRHGSDPGS), which is identical for known mammalian ERG1 channels, in the C terminus of the protein (Pond et al., 2000). Sections were deparaffinized, rehydrated, washed in PBS, permeabilized in 0.1% Triton X-100 for 25 min, and then incubated for 30 min in a blocking solution containing 1% bovine serum albumin and 1% goat serum. The 5 μm sections were incubated with rabbit anti-ERG1 antibody (Chemicon, Temecula, CA) overnight at 4°C. The rinsed sections were then incubated (6 h; 4°C) in FITC-conjugated goat anti-rabbit secondary antibody (Vector Laboratories, Burlingame, CA). Images were captured with an Olympus (Tokyo, Japan) BH-2 immunofluorescence microscope configured with a SPOT RT-KE CCD camera and SPOT image analysis software (Diagnostic Instruments, Sterling Heights, MI). Final figures were assembled with Adobe Photoshop software (Adobe Systems, San Jose, CA).

Immunoelectron microscopy

Young-adult 129Sv mice were transcardially perfused with 4% paraformaldehyde/0.1% glutaraldehyde in 0.1 M sodium cacodylate buffer, pH 7.4. The temporal bones were isolated, and the cochlea was perfused through the round and oval windows followed by immersion in fixative (1 h). The cochleas were stained with 2% osmium tetroxide (20 min; 23°C), decalcified (120 mM EDTA, pH 7.0; 24 h; 23°C), dehydrated through a graded alcohol series, and infiltrated with epoxy resin (Embed 812; Electron Microscopy Sciences, Fort Washington, PA). The polymerized blocks were bisected in the mid-modiolar plane. Ultrathin sections (70 nm), mounted on Formvar-coated nickel slot grids, were incubated on drops of 4% sodium metaperiodate, washed, and then floated on a blocking buffer solution containing 1% ovalbumin and 0.1% cold fish gelatin. The sections were incubated in rabbit anti-ERG (1:125) or blocking buffer only (48 h; 4°C), followed by six washes (10 min each). Sections were then floated on an anti-rabbit IgG conjugated with 10 or 16 nm colloidal gold (1:10; 1 h; 23°C; BBI International, Salida, CO). Finally, the sections were stained with uranyl acetate and lead citrate and viewed on a Jeol (Peabody, MA) 1010× transmission electron microscope. Digitized images were acquired and archived with an Orca CCD camera (Hamamatsu Photonics, Bridgewater, NJ) and AMT Advantage 12-HR software (version 5.4.2.239; Advanced Microscopy Techniques, Danvers, MA).

Heterologous expression in Xenopus *oocytes and mammalian cell line*

For heterologous expression in oocytes, MERG1a full-length cDNA was cloned into pNLE, in which MERG1a cDNA was flanked by 5′ and 3′ untranslated regions of a *Xenopus* β-globin gene (Nie et al., 2004). MERG1a RNA was prepared *in vitro* with T7 RNA polymerase (Ambion, Austin, TX) from the plasmid pNLR–MERG1a and injected into stage V–VI oocytes (Calvo et al., 1994). The full-length MERG1a cDNA was subcloned into a pIRES2–enhanced green fluorescent protein (EGFP) vector (Clontech, Cambridge, UK), which also encoded a GFP as a reporter. Plasmid DNA was isolated with Qiagen plasmid kits and transfected into CHO cells with the transfection reagent Lipofectamine 2000 (Invitrogen). Recordings were made from the transfected cells after 24 h.

Electrophysiological recordings

Recordings from ICs. To record from ICs, the lateral wall of the cochlear duct was removed from each inner ear while immersed in MEM solution (Invitrogen), pH 7.4, with 10 mM HEPES. The tissue was treated with the enzyme mixture for 15 min as described by Takeuchi et al. (1997). The epithelium was mounted in a custom-made chamber consisting of a cell-isolation and recording compartment, and the ICs were identified (pigmented ICs). The identified ICs were moved with a blunt pipette into a collagen-coated recording compartment of the chamber. Solutions consisted of the following (in mM): 80 *N*-methyl-D-glucamine (NMG), 40 choline, 10 Na^+, 3 K^+, 4 Ca^{2+}, 5 glucose, and 5 HEPES, pH 7.4 (NaOH). The pipette solutions contained (in mM): 130 K-glutamic acid, 10 KCl, 10 EGTA, 10 HEPES, and 5 ATP, pH 7.2 (KOH).

Recordings from heterologous expression systems. Oocytes were voltage clamped with a two-microelectrode amplifier (Warner Instruments, Hamden, CT). Macroscopic K^+ currents were recorded in a bath solution containing (in mM): 96 NaCl, 2 KCl, 0.5 $MgCl_2$, and 5 HEPES, pH 7.6 (NaOH). For some experiments, external Na^+ (Na^+_e) was replaced with K^+ to increase the bath K^+ concentration. To block endogenous Ca^{2+}-activated Cl^- currents in oocytes, the bath solution contained 1 mM niflumic acid (Collier et al., 1996). The pipettes contained 3 M KCl. Oocytes expressing robust K^+ currents were transferred onto an inverted microscope after the vitelline membrane had been peeled, and cell-attached or inside-out patches were excised to record single-channel activity.

Standard patch-clamp recording techniques (Hamill et al., 1981) were used to record whole-cell and single-channel currents from CHO cells with an Axopatch 200B amplifier (Molecular Devices, Union City, CA). The same amplifier was used to record single-channel currents from *Xenopus* oocytes expressing robust K^+ currents. In all experiments, the cell capacitance was calculated as the ratio of total charge (the integrated area under the current transient) to the magnitude of the pulse (20 mV). The series resistance was compensated electronically. For single-channel recording, the amplitude histogram at a given test potential was generated. Leak-subtracted current recordings were idealized with a half-height criterion. The bath solution contained (in mM): 140 NMG, 4 KCl,

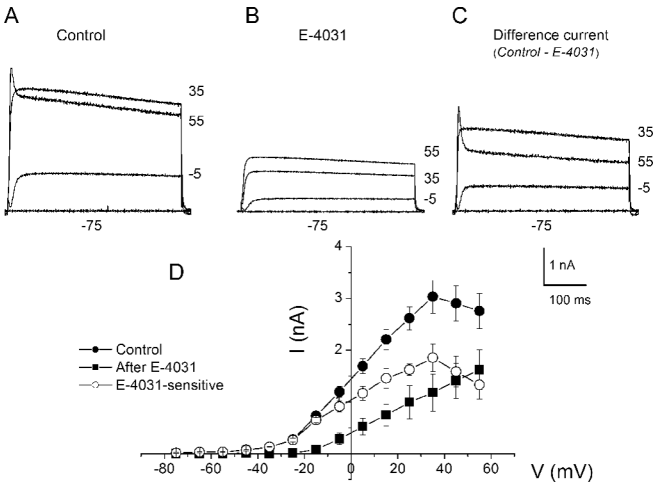

Figure 1. Whole-cell K^+ currents recorded from intermediate cells of the stria vascularis of the mouse. ***A***, Representative traces for a family of K^+ currents obtained from a holding potential of −80 mV and stepped up to the voltages indicated. Inward sodium and calcium currents, if present, were suppressed by substituting choline and NMG for sodium and calcium ions (see Materials and Methods). ***B***, Similar data obtained from the same cell (***A***) after application of external solution containing 1 μM E-4031, a delayed rectifier K^+ current blocker. ***C***, Difference current traces (***A***, ***B***) depicting the E-4031-sensitive current traces. For clarity, most of the current traces were not plotted. ***D***, Summary data of the current–voltage relationship of control (●), current after application of E-4031 (■), and the E-4031-sensitive component (○). The mean steady-state current magnitudes at ~300–400 ms were measured at the different test potentials. The data represent recordings from seven intermediate cells.

2 $CaCl_2$, 1 $MgCl_2$, and 10 HEPES, pH 7.4 (methanesulfonic acid). The internal solution contained (in mM): 130 K-glutamic acid, 10 KCl, 10 EGTA, 10 HEPES, and 5 ATP, pH 7.2 (KOH). Unless indicated otherwise, all chemicals were purchased from Sigma-Aldrich (St. Louis, MO). The methanesulfonanilide drug E-4031 and the recombinant peptide rBeKm-1 were purchased from Alomone Labs (Jerusalem, Israel). For single-channel recordings, patch electrodes contained (in mM): 140 KCl, 0.5 $MgCl_2$, 1 $CaCl_2$, 5 HEPES, and 10 D-glucose, pH 7.4 (KOH). The bath solution contained (in mM): 140 KCl, 4 NaCl, 1 $CaCl_2$, 0.5 $MgCl_2$, 5 HEPES, and 10 D-glucose, pH 7.4 (KOH). All experiments were performed at room temperature (22–23°C). Data are expressed as mean ± SD. The Q-software was used for single-channel analysis, as described previously (Rodriguez-Contreras and Yamoah, 2001, 2003; Rodriguez-Contreras et al., 2002).

Results

Identification of ERG-channel currents in intermediate cells

Intermediate cells from the StV express K^+ currents with features that are consistent with ERG-channel currents. As shown in Figure 1, K^+ currents elicited from a holding potential of −80 mV and stepped up to 55 mV were sustained at low-activation voltages; however, at high-activation voltages, the current showed a tendency toward inward rectification. Because the current phenotype was reminiscent of ERG-channel-type currents (London et al., 1997), we examined the sensitivity of the delayed rectifier K^+ (I_{Kr}) current toward E-4031 (Fig. 1*B*). The difference current (Fig. 1*C*) and the summary data shown in the current–voltage curves in Figure 1*D* reveal an E-4031-sensitive component, suggesting that ICs may express an ERG K^+ channel subtype. Motivated by these findings, we cloned ERG channels from the mouse inner ear.

Cloning of cochlear lateral wall MERG1a

MERG1a transcript was detected in the mouse inner ear by RT-PCR, with RNA isolated from the StV and the OC and primers specific for mouse heart MERG1a (GenBank accession number AF012868); RNA from mouse brain and heart were used as positive controls. A band with the expected size (1386 bp) was obtained from both the OC and the StV, respectively (Fig. 2). The full-length MERG1a cDNA from mouse StV was assembled from three PCR clones (mergE1, mergE2, and mergE3; data not shown) and sequenced with overlapped primers. Sequence analysis identified MERG1a cDNA from the mouse inner ear (GenBank accession number AY374424) that was 3499 bp long, and

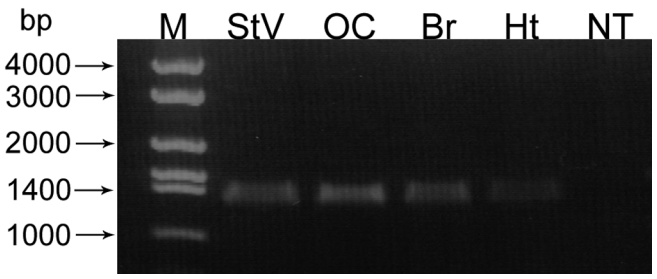

Figure 2. RT-PCR for detecting MERG1a expression in the inner ear. RNA from different tissues was used. A band at ~1.4 kb was obtained for all tested RNA samples. M, DNA molecular weight; StV, stria vascularis; OC, organ of Corti; Br, brain; Ht, heart; NT, no RNA template control.

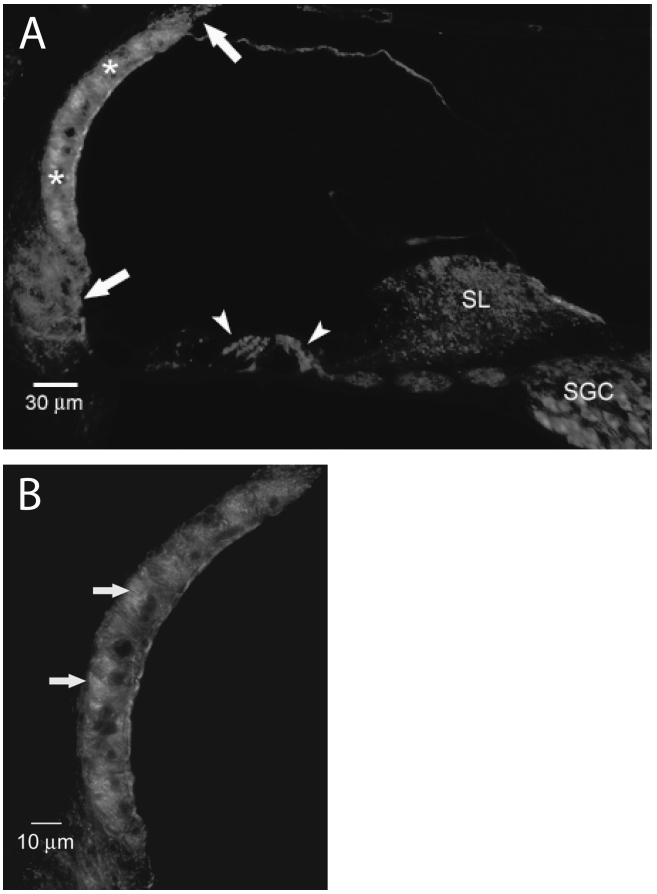

Figure 3. Reactivity for ERG in a cross section of a lower apical turn of a mouse cochlea. ***A***, Immunoreactivity for ERG is localized to the middle portion of the stria vascularis (asterisks). Lower levels of reactivity are noted in the spiral ganglion cells and outer and inner hair cells (arrowheads), as well as below and above the stria vascularis in the region of the type II and type V fibrocytes (arrows), respectively. ***B***, Higher magnification of the stria vascularis shows that the immunoreactivity is localized to the region of the interdigitating processes of marginal and intermediate cells, although the apical margin of some marginal cells is also reactive. SL, Spiral ligament; SGC, spiral ganglion cell.

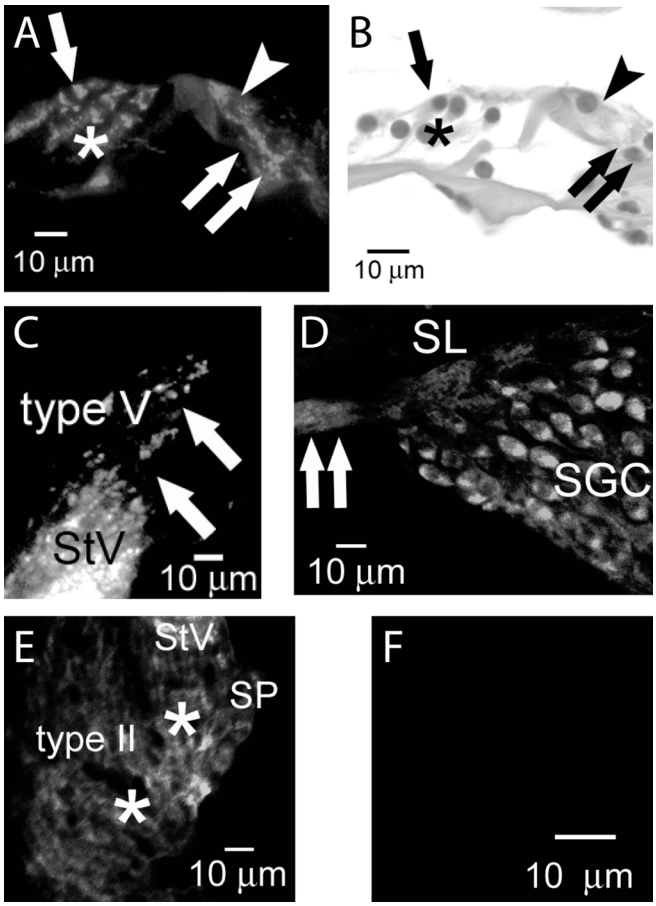

Figure 4. Reactivity for ERG in nonstrial cochlear tissue. ***A***, ***B***, Organ of Corti. The specificity of the ERG reactivity in the hair cells is shown in ***A***; an adjacent section stained with hematoxylin is shown in ***B***. Reactivity in the outer hair cells is most pronounced in the perinuclear region (arrow), whereas reactivity is noted throughout the cytoplasm of the inner hair cell (arrowhead). The cups of the Dieter's cells (asterisks) also appear immunofluorescent. ERG is expressed in the eighth nerve fibers under the inner hair cell (double arrows). ***C***, ***E***, Immunofluorescence in the spiral ligament was confined to the type II fibrocytes in the region of the spiral prominence and surrounding the root cells (asterisks) as well in the superficial layer of the type V fibrocytes (arrows) superior to the stria vascularis. ***D***, Rosenthal's canal (double arrows) as well as the spiral ganglion cells of the modiolus are reactive for ERG. ***E***. A cross section of a basal turn lateral wall from a mouse cochlea in which normal serum was substituted for the primary antibody lacks reactivity for ERG. OHC, Outer hair cell; SGC, spiral ganglion cell; SL, spiral limbus; SP, spiral prominence. ***F***, Negative control.

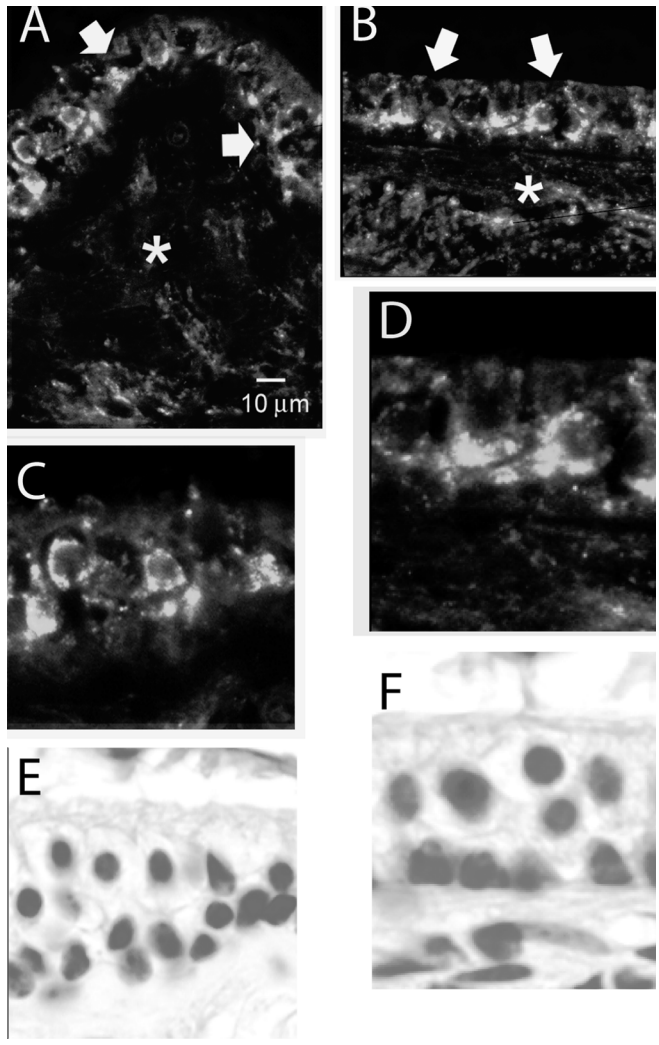

Figure 5. Reactivity for ERG in vestibular tissue. ***A***, ***B***, Immunoreactivity for ERG is localized to the hair cells (arrows) and nerve fibers (asterisks) in both the crista ampullaris (***A***) and the macula (***B***). ***C***, ***D***, A view of the sensory epithelium at higher magnification indicates ERG reactivity in the basal pole of the hair cells. The staining often shows a punctuate perinuclear pattern. Whether ERG is confined to the hair cell or is also present in the nerve calyx cannot be determined at the light microscopic level. ***E***, ***F***, Adjacent sections at the same magnification stained with hematoxylin.

the conserved Kozaka sequence was added to this cDNA by a specially designed primer to facilitate the expression of the channel. The deduced MERG1a protein, which is 1162 aa in length, contains the functional domains that have been described previously (Coetzee et al., 1999), including six transmembrane domains and the putative pore-forming region. Comparison of amino acid sequences shows that this channel protein shares high homology with ERG1a proteins from other tissue types and species (London et al., 1997; Pond et al., 2000).

Expression of MERG1a in the inner ear

To examine the expression pattern of MERG1a in the inner ear, we used immunofluorescence microscopy to detect and localize the protein in mid-modiolar sections. In the cochlear lateral wall, positive immunoreactivity for ERG was localized to the StV (Fig. 3) and the regions of the type II and type V fibrocytes (Figs. 3, 4). In the OC, the outer and inner hair cells showed reactivity. The reactivity was most intense at the basal pole, particularly for the outer hair cells (Figs. 3, 4). Finally, strong reactivity was noted in the spiral ganglion cells (Figs. 3, 4). At higher magnification, the immunofluorescent reactivity for ERG in the StV could be localized to the region of the interdigitating processes of MCs and ICs. The location of ERG in vestibular tissue was also assessed. As shown in Figure 5, immunofluorescent label was noted in vestibular hair cells of both the saccule and the crista ampullaris. In addition, the vestibular nerve fibers under the hair cells in both end organs were also reactive for ERG. Positive labeling was absent when tissue sections were preincubated with purified peptides (Fig. 4*E*).

The exact location of MERG1a in cells of the cochlear duct was investigated with postembedding immunogold transmission electron microscopy. Figure 6 shows cell-specific localization of gold particles in the cochlear lateral wall. The cytoplasm and the interdigitating processes of the ICs of the StV showed scattered gold label (Fig. 6*A*,*B*). Occasional particles were noted on the plasmalemma of MCs. Under the StV, the type II fibrocytes showed sparse labeling (Fig. 6*C*). At the light microscopic level,

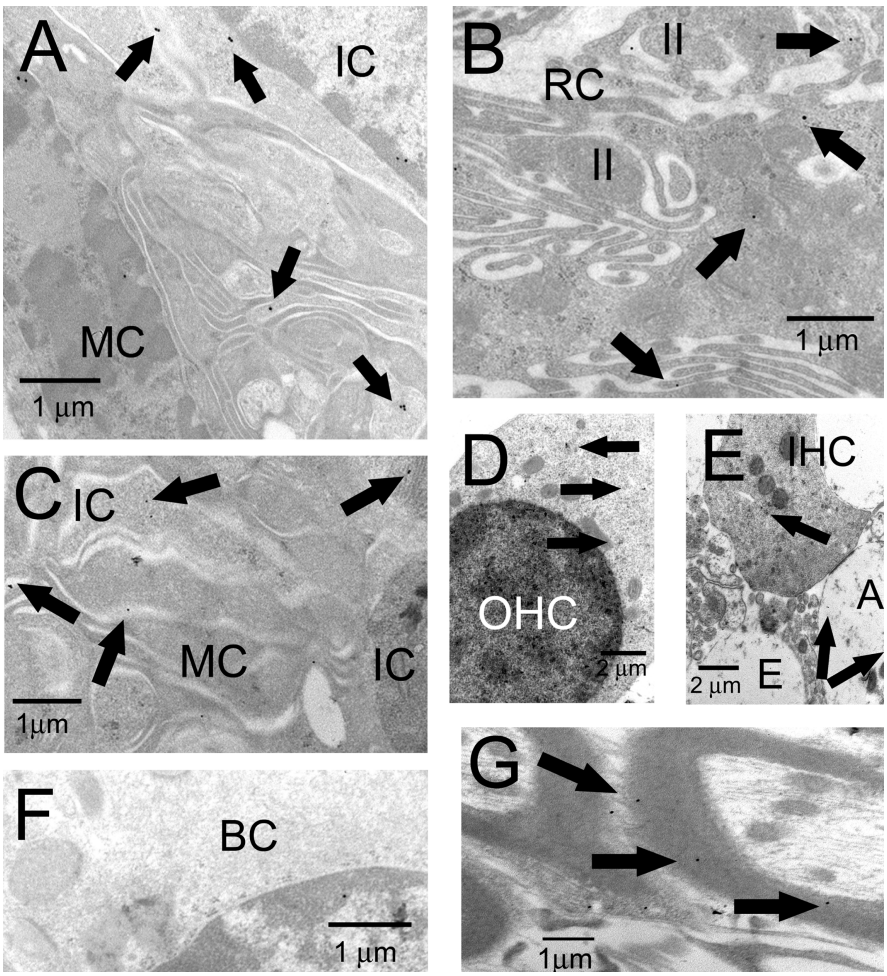

Figure 6. Immunogold localization of MERG. Cochlear sites of MERG expression were examined with immunogold electron microscopy with the postembedding technique. Thin mid-modiolar sections (70 nm) of cochlea used previously for routine ultrastructural examination were etched with sodium metaperiodate before incubation in primary and secondary antibodies conjugated to either 16 nm (***A***, ***F***, ***G***) or 10 nm (***B–E***) colloidal gold particles (arrows). ***A***, ***C***, In the stria vascularis, particles were localized in the cytoplasm and processes of the intermediate cells. Occasional particles were noted on the plasmalemma of marginal cells. The number of particles on intermediate cell interdigitations or cytosol around the nucleus exceeds the label on the marginal cell processes by ~40–45%. Label was seen only in the processes that extend into the interstrial space; no label was seen on the cell body of the marginal cells. Of the marginal or intermediate cells (***A***, ***C***), 90–95% of the specific label is adjacent to or near the plasmalemma, and, in a few instances, several gold particles are clumped together and it is impossible to determine which cell type they localize. ***B***, In the spiral ligament, labeling was found on the type II fibrocytes in the region in which their amplified processes were interspersed with the upper root cells. ***D***, The area immediately above the nucleus of the outer hair cell showed some gold particles. ***E***, In the inner hair cell, however, gold label was observed at the base of the hair cell and in the cytosol of afferent fibers. A, Afferent nerve; E, efferent nerve. ***G***, Gold particles were also found in nerve fibers in Rosenthal's canal. ***F***, However, no particles were observed in the cytosol or plasmalemma of the basal cells of the stria vascularis. The nuclear location of gold particles may be nonspecific binding associated with the colloidal gold technique (Smith and Jarett, 1993). RC, Root cell; II, type II fibrocytes.

the basal pole of the outer hair cells showed immunoreactivity (Fig. 4*B*); however, the labeling at the ultrastructural level was confined to the supranuclear area, as shown in Figure 6*D*. In contrast, gold particles were noted at the base of the inner hair cell (Fig. 6*E*). The labeling noted in the radial fibers under the inner hair cell extended into the nerve fibers in Rosenthal's canal.

Macroscopic and pharmacologic properties of MERG1a in the cochlear duct

Injection of MERG1a RNA into *Xenopus* oocytes yielded the expression of an outward K^+ current that activated at approximately of −50 mV, reaching a peak at ~10 mV and rectifying inwardly at step potentials >10 mV. Figure 7, *A* and *B*, shows that although uninjected oocytes did not express any appreciable outward current, oocytes injected with MERG1a channel RNA expressed macroscopic outward K^+ currents. The average maximum current recorded at a step voltage of 0 mV was 2.2 ± 0.3 μA ($n = 19$). The tiny current recorded from uninjected oocytes is most likely a leak current because it reverses at ~0 mV (Fig. 7*C*). Detailed analyses of the kinetics of HERG1a currents have demonstrated that the apparent inward rectification of the current at positive potentials reflects the rapid onset of inactivation (Trudeau et al., 1995; Spector et al., 1996). The inactivation of the channel apparently develops faster than activation at depolarized voltage steps (Spector et al., 1996). Thus, the optimum operating voltage ranges of the channel as an outward current lie within approximately −50 to 10 mV. Tail current traces recorded from 10 oocytes were used to determine the steady-state activation curve (Fig. 7*D*). This curve was fitted with a Boltzmann function with a $V_{1/2}$ (−47.4 ± 1.4 mV; $n = 10$) value and slope factor (10.6 ± 1.3 mV) that were similar to those reported for HERG currents and delayed rectifier K^+ currents (Shibasaki, 1987; Sanguinetti and Jurkiewicz, 1990; Faravelli et al., 1996; Arcangeli et al., 1997).

Consistent with a MERG1a channel, the current was sensitive to E-4031 (Jurkiewicz and Sanguinetti, 1993; Smith et al., 1996). Application of 10 μM E-4031 completely blocked the outward K^+ current (peak current at a step potential of 10 mV after application of 10 μM E-4031 was 0.004 ± 0.003 μA; $n = 7$). The effect of 100 nM E-4031 on inner ear MERG1a channels expressed in oocytes is shown in Figure 8*A*. The currents were also sensitive to rBeKm-1, a known potent blocker of ERG1 channels (Korolkova et al., 2001) (Fig. 8*B*). The IC_{50} obtained for E-4031 was ~165 nM (Fig. 8*C*), whereas the IC_{50} for rBeKm-1 was ~16 nM (Fig. 8*D*).

One of the characteristic properties of I_{Kr} that has been ascribed to ERG current is its modulation by external K^+ concentrations ($[K^+]_e$) (Sanguinetti and Jurkiewicz, 1992). In contrast to other K^+ currents, in which increased $[K^+]_e$ results in a reduction in the electrochemical driving force and a decrease in the current magnitude, MERG1a current was enhanced by $[K^+]_e$ (Fig. 9*A–C*). The decay of the current was reduced as the Na^+_e was replaced with K^+. This is in keeping with reports that have demonstrated that the inactivation of ERG channel currents is mediated in part by blockage of Na^+_e (Numaguchi et al., 2000; Mullins et al., 2002). The relationship between $[K^+]_e$ and MERG1a current measured at different step potentials is shown in Figure 9*D*. This anomalous feature of MERG1a cur-

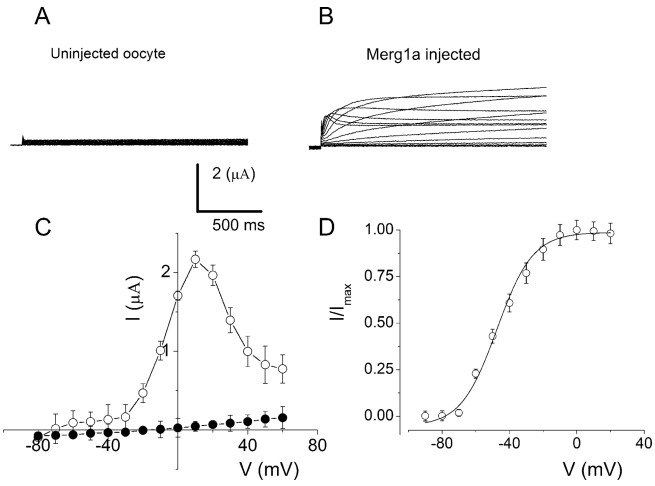

Figure 7. Expression of inner ear-specific MERG1a in *Xenopus* oocytes. Outward K^+ currents from *Xenopus* oocytes were injected with mRNA of StV-specific MERG1a channel. The recordings were obtained from a holding potential of −80 mV to step potentials ranging from −70 to +60 mV ($\Delta V = 10$ mV). ***A***, Uninjected oocytes had no current. ***B***, MERG1a-injected oocytes yielded robust currents. ***C***, Summary data of the current–voltage relationships from 19 oocytes. ***D***, Outward tail currents were elicited from different step potentials to −40 mV. The activation curve was obtained by plotting the normalized tail current (I/I_{max}) at each test potential and then fitted by the Boltzmann equation $\{I/I_{max} = [1 + \exp(V_{1/2} - V)/k_m]\}^{-1}$, where $V_{1/2}$ is the half-activation voltage and k_m is the maximum slope. The estimated $V_{1/2}$ and k_m from the activation curve were −47.4 ± 1.4 and 10.6 ± 1.3 mV ($n = 10$), respectively.

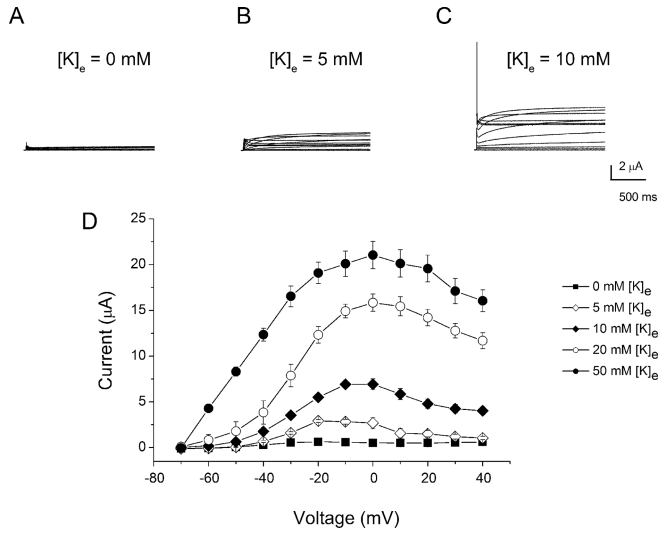

Figure 9. Effects of $[K^+]_e$ on the magnitude of MERG1a currents. ***A***, Exemplary MERG1a current traces elicited from a holding potential of −80 mV to step potentials ranging from −80 to +40 mV with $\Delta V = 10$ mV. The current was recorded in an external solution with no added K^+ (~0 mM). ***B***, ***C***, Similar current traces elicited after perfusing external solutions containing 5 and 10 mM K^+, respectively. Unlike most K^+ currents, the current magnitudes increase with increasing $[K^+]_e$. Group summary data of the MERG1a current magnitude versus voltage at different $[K^+]_e$ (0–50 mM; $n = 7$) are shown. The currents were substantially enhanced as $[K^+]_e$ was increased.

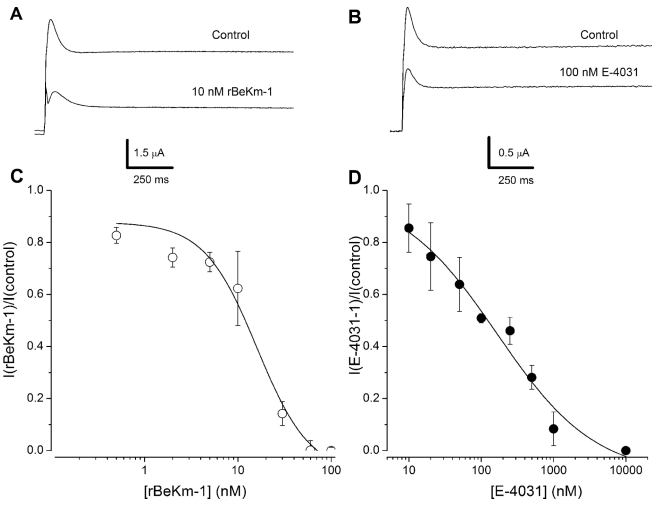

Figure 8. Pharmacology of inner ear-specific MERG1a. Outward K^+ current from *Xenopus* oocytes injected with mRNA of StV-specific MERG1a channel was sensitive to rBeKm-1 and E-4031. ***A***, ***B***, Examples of current traces recorded from a holding potential of −80 mV to a step potential of 30 mV for control and after application of rBeKm-1 and E-4031, respectively. The concentrations of the drugs are indicated. ***C***, ***D***, Dose–response curves. The IC_{50} values for rBeKm-1 and E-4031 were ~16 and 165 nM, respectively.

rent raises the physiological importance of the channel as a predominant factor in the net K^+ current under conditions of increased $[K^+]_e$.

Microscopic properties of MERG1a in the cochlear duct

Single-channel recordings were obtained from CHO cells transfected with MERG1a by using GFP as a reporter gene. To estimate the values of the voltage steps in the cell-attached configurations, cells were bathed in solutions containing high K^+ to clamp the membrane potential at ~0 mV. As shown in Figure 10*A*, the resulting single-channel fluctuations in symmetrical bath and patch-pipette K^+-containing solution exhibited inward current fluctuations at test potentials negative to the apparent reversal potential at ~0 mV. An example of the amplitude histograms used to determine the unitary current amplitude is shown in Figure 10*B*. The estimated single-channel conductance from the regression line of the current–voltage relationship in Figure 10*C* was 14.3 ± 2.8 pS ($n = 6$).

Discussion

Inner ear hair cells are designed and placed in a milieu that allows them to respond to mechanical displacements as minute as ~1 nm (Russell et al., 1989). An attribute of hair-cell sensitivity is derived partly from the EP. Because of the EP, a robust direct current potential of ~140 mV [approximately 60 mV (the resting membrane potential of hair cells) plus ~80 mV EP] generates a standing current, which is the basis for the mechanoelectrical "battery theory" of cochlear transduction (Von Bekesy, 1950). The EP is generated by the high K^+ throughput across the IC membrane (Salt et al., 1987), leading to the exceptionally high K^+ concentration ($[K^+]$) in the endolymph (~150 mM). Although there is a substantial outward component of Kir4.1 channel currents in the ICs (Takeuchi et al., 2000; Nie et al., 2005), the predicted potential sensed by the protein or any other K^+ channel (approximately −100 mV) (Takeuchi et al., 2000) will produce a resulting inward current, which underpins the need for a refinement of the prevailing model for the generation of the EP. Clearly, the sustained outflow from the ICs and the uptake from the IS are essential for the generation and maintenance of the EP. Moreover, several landmark reports have shown that K^+ exits the StV through the apical membrane of MCs via K^+ channels, driven by the apical membrane potential, which is at least 10 mV more positive than EP (Salt et al., 1987; Vetter et al., 1996; Wangemann, 2002; Casimiro et al., 2004). In contrast, Cl^- ions are removed from MCs via the basolateral membrane Cl^- channels, ClC-K1 and ClC-K2 (Oshima et al., 1997; Sage and Marcus,

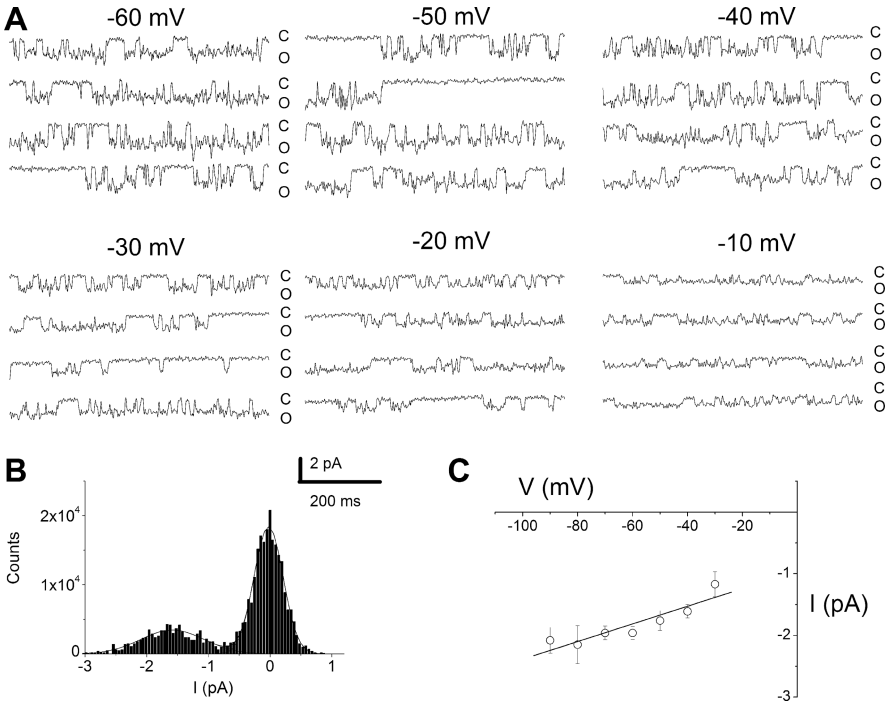

Figure 10. Single-channel currents of MERG1a expressed in CHO cells. ***A***, Representative and consecutive single-channel traces recorded in a cell-attached patch with a pipette ($[K^+]$, 140 mM). The bath solution contained 140 mM K^+, and the resting potential of CHO cells was ~0 mV. The holding potential was −50 mV, and the step potentials are indicated. The *I–V* relationships are shown in ***B***. The inset in ***B*** is an example of an amplitude histogram used to generate *I–V* relationships at 50 mV. The single-channel conductance was 14.3 ± 2.8 pS ($n = 6$). C, Closed; O, open.

2001). The $[K^+]$ in the endolymphatic space and EP maintenance depend on several dynamic processes and the structure of the cochlear duct: (1) the active secretion of K^+ ions from the StV, (2) K^+ extrusion from the endolymph through transduction channels of hair and spiral ligament cells (Schulte and Schmiedt, 1992; Spicer and Schulte, 1998), and (3) the tight junctions between cells in the StV (Jahnke, 1980) and the ensuing impedance. Thus, K^+ cycling in the cochlear duct maintains the high throughput of K^+ across BC–IC membranes, which confers the EP (Salt et al., 1987). This process is essential for normal cochlear function because it prevents K^+ accumulation in the perilymph of hair cells and curtails untoward membrane depolarization.

Thus far, the K^+ channels that establish the K^+ flux across IC membranes remain uncertain. Although it is thought that a key channel involved in the outward K^+ movement across the IC membrane is the Kir4.1 channel (Takeuchi et al., 2000; Marcus et al., 2002), this circumstantial evidence presents a biophysical paradox: Kir4.1 is an inwardly rectifying K^+ channel (Hille, 2001). Indeed, a recent report suggests that Kir4.1 in the inner ear may operate to control the resting membrane potential of ICs and perhaps reduce the $[K^+]$ in the IS of the StV (Nie et al., 2004). Consequently, the identity of the K^+ channels that confer EP across ICs should be sought.

To our knowledge, this study constitutes the first report on the functional and molecular identification of MERG1a and its specific localization in the StV and extrastrial cells in the inner ear, and it determines the biophysical and pharmacologic features of the channel. First cloned from the cDNA library of the hippocampus by homology to *ether-a-go-go*, a *Drosophila* K^+ channel gene (Warmke and Ganetzky, 1994), the channel has been identified in several tissues, including neurons (Emmi et al., 2000; Gullo et al., 2003) and muscle (Shoeb et al., 2003); however, only the high expression of the HERG protein in cardiac myocytes and the significant role of the channel current in the plateau phase of the cardiac action potential have been studied exhaustively (Curran et al., 1995). The importance of HERG protein in cardiac function is underpinned by the fact that mutations in the channel, as well as drugs blocking the current, result in long QT syndrome (Curran et al., 1995; Vandenberg et al., 2001).

MERG1a in the inner ear is a 1162 aa protein with six transmembrane domains and a Glu–Phe–Glu signature sequence in the P-loop that defines K^+ channels (Tinker et al., 1996). The amino acid sequence of the inner ear MERG1a bears a striking resemblance to ERG1a channel in mouse heart (99%), rabbit heart (95%), rat heart (98%), and human heart (95%) (London et al., 1997; Pond et al., 2000), suggesting that the properties of the current, of at least the α-subunit, may have a similar biophysical and pharmacologic phenotype. The current derived from the α-subunit expressed in heterologous expression systems is consistent with the I_{Kr} component of delayed rectifier K^+ currents (Sanguinetti and Jurkiewicz, 1990; Abbott et al., 1999); however, some reports indicate that the α-subunit alone may not suffice to recapitulate the native I_{Kr} phenotype (Sanguinetti et al., 1995). MiRP1, encoded by *KCNE2*, has been shown to coassemble with the HERG subunit to confer the features of I_{Kr}, and mutations in KCNE2 have been linked to long QT syndrome (Abbott et al., 1999; Zhang et al., 2001; Weerapura et al., 2002).

The channel is abundantly expressed in ICs, raising the possibility that MERG1a may serve a specific role in the StV. The location of ERG channel in the plasmalemma of the IC ensures a high K^+ flux from ICs into the IS. This may result in a steep K^+ gradient, the maintenance of which requires a sustained current. Although the sharp concentration difference between ICs and the IS may be facilitated by K^+ uptake mechanisms by Na–K pumps and Na–K–Cl cotransporters (NKCC1) in the basolateral membrane of MCs (Flagella et al., 1999), the activation and inactivation properties of MERG1a should be poised to regulate K^+ extrusion from ICs and $[K^+]$ in the IS. The positive slope conductance at approximately −50 to 10 mV and the negative slope conductance at potentials positive to 10 mV is a property critical for limiting outward K^+ flux to establish the gradient required to establish EP.

MERG1a in ICs and hair cells may be even more important in K^+ extrusion. Because of the tight junctions among MCs, BCs, and endothelial cells in the StV (Jahnke, 1980) and presumably the high K^+ flux across ICs, the IS constitutes a separate fluid compartment with ~13 mM K^+ (Salt and Thalmann, 1988) (but see Takeuchi et al., 2000). For a classic K^+ channel, the electrochemical driving force for outward K^+ flux from ICs is expected to decrease by ~30 mV. Because elevation of external K^+ causes an increase in outward MERG1a current (Fig. 9), the physiological implication of this paradoxical phenotype of the channel could be vast in the StV. MERG1a current should be the predominant outward K^+ current in ICs, but the data cannot rule out the

possibility that MERG1a may be expressed in MCs as well. Functionally, however, we argue that MERG1a may play a restricted role in K^+ extrusion in MCs, because the channel shows strong inward rectification at potentials positive to ~10 mV (Fig. 7*C*). Because the membrane potential sensed by the channels at the apical membrane of MCs is ~10 mV [the membrane potential of MCs with respect to ground is approximately +90 mV (Salt et al., 1987)], MERG1a may not produce a strong outward current in MCs. Rather, MERG1 may play an essential role in the extrusion of K^+ in ICs of the StV. Moreover, during prolonged stimulation of hair cells and/or ischemic conditions, K^+ may accumulate in the intercellular space (Kharkovets et al., 2000). These conditions of elevated external K^+ concentrations would be expected to increase the contribution of MERG1a current to the repolarization of hair cells. It has been suggested that a low-voltage-activated K^+ conductance, $g_{K,L}$, in vestibular hair cells may have pharmacologic properties that are consistent with ERG channels (Wong et al., 2004). The expression of MERG1a, a channel with a distinct K^+-conducting behavior (Fig. 9), in calyx afferent endings may be even more important, given that the synaptic cleft is prone to increased K^+ accumulation during enhanced excitability (Goldberg, 1996; Wong et al., 2004); however, the expression and functional import of MERG1 in the sensory epithelium of the vestibule require further studies.

The expression of ERG in type II and type V fibrocytes of the spiral ligament is consistent with the concept that K^+, which leaks from the scala media, is actively recycled from the OC, scala vestibuli, and tympani by the lateral wall fibrocytes. The presence of ERG channels could complement the activities of the Na–K pump and the Na–K–Cl cotransporter, which are present in type II and type V fibrocytes (Schulte and Schmiedt, 1992; Crouch et al., 1997), in establishing a K^+ flux toward StV BCs through the type I fibrocytes.

References

Abbott GW, Sesti F, Splawski I, Buck ME, Lehmann MH, Timothy KW, Keating MT, Goldstein SA (1999) MiRP1 forms I_{Kr} potassium channels with HERG and is associated with cardiac arrhythmia. Cell 97:175–187.

Arcangeli A, Rosati B, Cherubini A, Crociani O, Fontana L, Ziller C, Wanke E, Olivotto M (1997) HERG- and IRK-like inward rectifier currents are sequentially expressed during neuronal development of neural crest cells and their derivatives. Eur J Neurosci 9:2596–2604.

Calvo DJ, Vazquez AE, Miledi R (1994) Cationic modulation of rho 1-type gamma-aminobutyrate receptors expressed in *Xenopus* oocytes. Proc Natl Acad Sci USA 91:12725–12729.

Carlisle L, Steel K, Forge A (1990) Endocochlear potential generation is associated with intercellular communication in the stria vascularis: structural analysis in the viable dominant spotting mouse mutant. Cell Tissue Res 262:329–337.

Casimiro MC, Knollmann BC, Yamoah EN, Nie L, Vary JC, Surenko S, Greene AE, Grinberg A, Huang SP, Ebert SN, Pfeifer K (2004) Targeted point mutagenesis of mouse Kcnq1: phenotypic analysis of mice with point mutations that cause Romano-Ward syndrome in humans. Genomics 84:555–564.

Coetzee WA, Amarillo Y, Chiu J, Chow A, Lau D, McCormack T, Moreno H, Nadal MS, Ozaita A, Pountney D, Saganich M, Vega-Saenz de Miera E, Rudy B (1999) Molecular diversity of K^+ channels. Ann NY Acad Sci 868:233–285.

Collier ML, Levesque PC, Kenyon JL, Hume JR (1996) Unitary Cl^- channels activated by cytoplasmic Ca^{2+} in canine ventricular myocytes. Circ Res 78:936–944.

Crouch JJ, Sakaguchi N, Lytle C, Schulte BA (1997) Immunohistochemical localization of the Na-K-Cl co-transporter (NKCC1) in the gerbil inner ear. J Histochem Cytochem 45:773–778.

Curran ME, Splawski I, Timothy KW, Vincent GM, Green ED, Keating MT (1995) A molecular basis for cardiac arrhythmia: HERG mutations cause long QT syndrome. Cell 80:795–803.

Ehrlich JR, Pourrier M, Weerapura M, Ethier N, Marmabachi AM, Hebert TE, Nattel S (2004) KvLQT1 modulates the distribution and biophysical properties of HERG: a novel alpha-subunit interaction between delayed rectifier currents. J Biol Chem 279:1233–1241.

Emmi A, Wenzel HJ, Schwartzkroin PA, Taglialatela M, Castaldo P, Bianchi L, Nerbonne J, Robertson GA, Janigro D (2000) Do glia have heart? Expression and functional role for *ether-a-go-go* currents in hippocampal astrocytes. J Neurosci 20:3915–3925.

Faravelli L, Arcangeli A, Olivotto M, Wanke E (1996) A HERG-like K^+ channel in rat F-11 DRG cell line: pharmacological identification and biophysical characterization. J Physiol (Lond) 496:13–23.

Flagella M, Clarke LL, Miller ML, Erway LC, Giannella RA, Andringa A, Gawenis LR, Kramer J, Duffy JJ, Doetschman T, Lorenz JN, Yamoah EN, Cardell EL, Shull GE (1999) Mice lacking the basolateral Na-K-2Cl cotransporter have impaired epithelial chloride secretion and are profoundly deaf. J Biol Chem 274:26946–26955.

Goldberg JM (1996) A theoretical analysis of intercellular communication between the vestibular type 1 hair cell and its calyx ending. J. Neurophysiol 76:1942–1957.

Gullo F, Ales E, Rosati B, Lecchi M, Masi A, Guasti L, Cano-Abad MF, Arcangeli A, Lopez MG, Wanke E (2003) ERG K^+ channel blockade enhances firing and epinephrine secretion in rat chromaffin cells: the missing link to LQT2-related sudden death? FASEB J 17:330–332.

Hamill OP, Marty A, Neher E, Sakmann B, Sigworth FJ (1981) Improved patch-clamp techniques for high-resolution current recording from cells and cell-free membrane patches. Pflügers Arch 391:85–100.

Hibino H, Horio Y, Inanobe A, Doi K, Ito M, Yamada M, Gotow T, Uchiyama Y, Kawamura M, Kubo T, Kurachi Y (1997) An ATP-dependent inwardly rectifying potassium channel, KAB-2 (Kir4.1), in cochlear stria vascularis of inner ear: its specific subcellular localization and correlation with the formation of endocochlear potential. J Neurosci 17:4711–4721.

Hille B (2001) Ion channels of excitable membranes. Sunderland, MA: Sinauer.

Hudspeth AJ (1992) Hair-bundle mechanics and a model for mechanoelectrical transduction by hair cells. Soc Gen Physiol Ser 47:357–370.

Jahnke K (1980) The blood–perilymph barrier. Arch Otorhinolaryngol 228:29–34.

Jurkiewicz NK, Sanguinetti MC (1993) Rate-dependent prolongation of cardiac action potentials by a methanesulfonanilide class III antiarrhythmic agent: specific block of rapidly activating delayed rectifier K^+ current by dofetilide. Circ Res 72:75–83.

Kharkovets T, Hardelin JP, Safieddine S, Schweizer M, El-Amraoui A, Petit C, Jentsch TJ (2000) KCNQ4, a K^+ channel mutated in a form of dominant deafness, is expressed in the inner ear and the central auditory pathway. Proc Natl Acad Sci USA 97:4333–4338.

Korolkova YV, Kozlov SA, Lipkin AV, Pluzhnikov KA, Hadley JK, Filippov AK, Brown DA, Angelo K, Strobaek D, Jespersen T, Olesen SP, Jensen BS, Grishin EV (2001) An ERG channel inhibitor from the scorpion *Buthus eupeus*. J Biol Chem 276:9868–9876.

London B, Trudeau MC, Newton KP, Beyer AK, Copeland NG, Gilbert DJ, Jenkins NA, Satler CA, Robertson GA (1997) Two isoforms of the mouse ether-a-go-go-related gene co-assemble to form channels with properties similar to the rapidly activating component of the cardiac delayed rectifier K^+ current. Circ Res 81:870–878.

Marcus DC, Wu T, Wangemann P, Kofuji P (2002) KCNJ10 (Kir4.1) potassium channel knockout abolishes endocochlear potential. Am J Physiol Cell Physiol 282:C403–C407.

McDonald TV, Yu Z, Ming Z, Palma E, Meyers MB, Wang KW, Goldstein SA, Fishman GI (1997) A minK-HERG complex regulates the cardiac potassium current I(Kr). Nature 388:289–292.

Mullins FM, Stepanovic SZ, Desai RR, George Jr AL, Balser JR (2002) Extracellular sodium interacts with the HERG channel at an outer pore site. J Gen Physiol 120:517–537.

Nie L, Song H, Chen MF, Chiamvimonvat N, Beisel KW, Yamoah EN, Vazquez AE (2004) Cloning and expression of a small-conductance Ca(2+)-activated K^+ channel from the mouse cochlea: coexpression with alpha9/alpha10 acetylcholine receptors. J Neurophysiol 91:1536–1544.

Nie L, Feng W, Diaz R, Gratton MA, Doyle KJ, Yamoah EN (2005) Functional consequences of polyamine synthesis inhibition by DFMO: cellular mechanisms for DFMO-mediated ototoxicity. J Biol Chem 280:15097–15102.

Numaguchi H, Johnson Jr JP, Petersen CI, Balser JR (2000) A sensitive mechanism for cation modulation of potassium current. Nat Neurosci 3:429–430.

Oshima T, Ikeda K, Furukawa M, Takasaka T (1997) Expression of voltage-dependent chloride channels in the rat cochlea. Hear Res 103:63–68.

Pond AL, Scheve BK, Benedict AT, Petrecca K, Van Wagoner DR, Shrier A, Nerbonne JM (2000) Expression of distinct ERG proteins in rat, mouse, and human heart: relation to functional I(Kr) channels. J Biol Chem 275:5997–6006.

Rodriguez-Contreras A, Yamoah EN (2001) Direct measurement of single-channel Ca(2+) currents in bullfrog hair cells reveals two distinct channel subtypes. J Physiol (Lond) 534:669–689.

Rodriguez-Contreras A, Yamoah EN (2003) Effects of permeant ion concentrations on the gating of L-type Ca^{2+} channels in hair cells. Biophys J 84:3457–3469.

Rodriguez-Contreras A, Nonner W, Yamoah EN (2002) Ca^{2+} transport properties and determinants of anomalous mole fraction effects of single voltage-gated Ca^{2+} channels in hair cells from bullfrog saccule. J Physiol (Lond) 538:729–745.

Russell IJ, Richardson GP, Kossl M (1989) The responses of cochlear hair cells to tonic displacements of the sensory hair bundle. Hear Res 43:55–69.

Sage CL, Marcus DC (2001) Immunolocalization of ClC-K chloride channel in strial marginal cells and vestibular dark cells. Hear Res 160:1–9.

Salt AN, Thalmann R (1988) Interpretation of endolymph flow results: a comment on "longitudinal flow of endolymph measured by distribution of tetraethylammonium and choline in scala media". Hear Res 33:279–284.

Salt AN, Melichar I, Thalmann R (1987) Mechanisms of endocochlear potential generation by stria vascularis. Laryngoscope 97:984–991.

Sanguinetti MC, Jurkiewicz NK (1990) Two components of cardiac delayed rectifier K^+ current: differential sensitivity to block by class III antiarrhythmic agents. J Gen Physiol 96:195–215.

Sanguinetti MC, Jurkiewicz NK (1992) Role of external Ca^{2+} and K^+ in gating of cardiac delayed rectifier K^+ currents. Pflügers Arch 420:180–186.

Sanguinetti MC, Jiang C, Curran ME, Keating MT (1995) A mechanistic link between an inherited and an acquired cardiac arrhythmia: HERG encodes the I_{Kr} potassium channel. Cell 81:299–307.

Schulte BA, Schmiedt RA (1992) Lateral wall Na,K-ATPase and endocochlear potentials decline with age in quiet-reared gerbils. Hear Res 61:35–46.

Shi W, Wymore RS, Wang HS, Pan Z, Cohen IS, McKinnon D, Dixon JE (1997) Identification of two nervous system-specific members of the *erg* potassium channel gene family. J Neurosci 17:9423–9432.

Shibasaki T (1987) Conductance and kinetics of delayed rectifier potassium channels in nodal cells of the rabbit heart. J Physiol (Lond) 387:227–250.

Shoeb F, Malykhina AP, Akbarali HI (2003) Cloning and functional characterization of the smooth muscle ether-a-go-go-related gene K^+ channel: potential role of a conserved amino acid substitution in the S4 region. J Biol Chem 278:2503–2514.

Smith PL, Baukrowitz T, Yellen G (1996) The inward rectification mechanism of the HERG cardiac potassium channel. Nature 379:833–836.

Smith RM, Jarett L (1993) Electron microscopic immunocytochemical approaches to the localization of ligands, receptors, transducers, and transporters. In: Handbook of endocrine research techniques (DePablo F, Scanes CG, Weintraub BD, eds), pp 227–264. New York: Academic.

Spector PS, Curran ME, Zou A, Keating MT, Sanguinetti MC (1996) Fast inactivation causes rectification of the I_{Kr} channel. J Gen Physiol 107:611–619.

Spicer SS, Schulte BA (1998) Evidence for a medial K^+ recycling pathway from inner hair cells. Hear Res 118:1–12.

Takeuchi S, Ando M, Irimajiri A (1997) Changes in the volume of marginal cells induced by isotonic "Cl^- depletion/restoration": involvement of the Cl^- channel and Na^+-K^+-Cl^- cotransporter. Hear Res 113:99–109.

Takeuchi S, Ando M, Kakigi A (2000) Mechanism generating endocochlear potential: role played by intermediate cells in stria vascularis. Biophys J 79:2572–2582.

Tinker A, Jan YN, Jan LY (1996) Regions responsible for the assembly of inwardly rectifying potassium channels. Cell 87:857–868.

Trudeau MC, Warmke JW, Ganetzky B, Robertson GA (1995) HERG, a human inward rectifier in the voltage-gated potassium channel family. Science 269:92–95.

Vandenberg JI, Walker BD, Campbell TJ (2001) HERG K^+ channels: friend and foe. Trends Pharmacol Sci 22:240–246.

Vetter DE, Mann JR, Wangemann P, Liu J, McLaughlin KJ, Lesage F, Marcus DC, Lazdunski M, Heinemann SF, Barhanin J (1996) Inner ear defects induced by null mutation of the *isk* gene. Neuron 17:1251–1264.

Von Bekesy G (1950) DC potentials and energy balance of the cochlear partition. J Acoust Soc Am 22:576–582.

Wangemann P (2002) K^+ cycling and the endocochlear potential. Hear Res 165:1–9.

Warmke JW, Ganetzky B (1994) A family of potassium channel genes related to *eag* in *Drosophila* and mammals. Proc Natl Acad Sci USA 91:3438–3442.

Weerapura M, Nattel S, Chartier D, Caballero R, Hebert TE (2002) A comparison of currents carried by HERG, with and without coexpression of MiRP1, and the native rapid delayed rectifier current: is MiRP1 the missing link? J Physiol (Lond) 540:15–27.

Wong WH, Hurley KM, Eatock RA (2004) Differences between the negatively activating potassium conductances of mammalian cochlear and vestibular hair cells. J Assoc Res Otolaryngol 5:270–284.

Yang J, Jan YN, Jan LY (1995) Control of rectification and permeation by residues in two distinct domains in an inward rectifier K^+ channel. Neuron 14:1047–1054.

Zhang M, Jiang M, Tseng GN (2001) minK-related peptide 1 associates with Kv4.2 and modulates its gating function: potential role as beta subunit of cardiac transient outward channel? Circ Res 88:1012–1019.